Schlieren visualization of transient vapor penetration and spreading angle of a prototype diesel direct-acting piezoelectric injector

R. Payri[1*], J. Gimeno[1], J.P. Viera[1], A.H. Plazas[2]
[1] CMT Motores Termicos. Universitat Politecnica de Valencia, Spain
rpayri@mot.upv.es, jaigigar@mot.upv.es, juavieso@upv.es

[2] GM R&D, Warren, MI, USA
alejandroherna.plazastorres@GM.COM

Abstract

In this research work, a prototype diesel common rail direct-acting piezoelectric injector has been employed to study the influence of the fuel injection rate shaping on spray behavior (vapor phase penetration) under evaporative non-reacting conditions. This state of the art injector allows a fully flexible control of the nozzle needle lift through a parameter referred to as piezo stack charge level, enabling various fuel injection rates typologies under a wide range of test conditions. The tests have been performed employing a novel continuous flow test chamber that allows an accurate control of temperature and pressure up to 1000 K and 15 MPa respectively. The transient evolution of the spray has been studied recording movies of the injection event with a fast camera in a controlled 2-pass Schlieren visualization setup.

The effects of ambient temperature, injection pressure and piezo stack charge level have been studied and results are presented. Data obtained is correlated to previous liquid length and injection rate measurements of the same injector. Results show, as expected for all cases, that instant vapor penetration rate is closely related to the instant injection rate. Also for all cases, results show that the piezo stack charge and injection pressure affect the vapor penetration and spreading angle in a similar way. Ambient temperature alone seems not to have an important effect on vapor penetration and spreading angle, mainly because the two temperatures evaluated are close enough not to cause an important variation in ambient density. From the results, this needle control feature has proven to be a very versatile tool to control the injection process.

Introduction

The injection process takes a determinant part in the global functioning of a direct injection diesel engine [1][2][3]. Several studies have been performed in last decades in order to predict the spray behavior as well as the development of numerical models, either based on physical assumptions or simply interpolating experimental data [3][4][5][6][7]. Furthermore, continuous effort in reducing fuel consumption and emissions is leading to new injection technologies. The last development of piezo-actuated injectors is the so called *direct acting system*, where a piezo actuator (stack) has direct control on the injector needle lift that allows for a fast and precise control of the fuel flow through the injector nozzle. This particular feature offers the engine designers a wide variety of injection strategies to think of. Therefore, a deep understanding of the injector performance in all the range of its operating possibilities has to be reached.

Although many studies have been performed to analyze the injection event using conventional servo-hydraulic injectors, only a few are discussing the effect of the partial needle lift on the injection process [8][9]. In order to develop a deeper understanding of the effect of partial needle lift on the atomization process, this research has carried out an experimental study to measure vapor phase penetration of the fuel spray produced by a direct acting injector, using a controlled Schlieren setup.

The study has been performed in a high temperature and high pressure test rig, capable of reaching 15 MPa ambient pressure and 1000 K ambient temperature. The large optical accesses and the wide test section permit studying the spray with high accuracy in a homogeneous temperature and nearly quiescent environment. In this work, different parameters have been varied: ambient temperature, ambient density, injection pressure and needle lift (piezo stack charge).

The article is structured in five parts, first the present introduction, next the experimental set-up with an explanation of the test rig and the optical hardware utilized, later the hardware and processing tools, then the main results and analysis are presented to finalize with the main conclusions of the paper.

* Corresponding author: rpayri@mot.upv.es

Experimental methodology and setup

The fuel injection system

A common-rail injection system was used. It is constituted by a high pressure pump and a conventional rail with a pressure regulator, which allows fuel injection under high (up to 200 MPa) and relatively constant pressure [2][3][10]. The injector temperature was kept close to 343 K using a special injector holder designed to have coolant flowing at a controlled temperature in direct contact with the injector body. This study was performed using commercial Diesel fuel with a density of 812 kg/m^3 (at 70º) and kinematic viscosity of 1.9 10^{-6} mm^2/s (at 70º). The fuel was injected through the previously described, prototype state of the art piezoelectric injector, with a 7-hole nozzle (Outlet diameter D_0 = *156 µm, k-factor = 1.5* [8]*)* which permits full control of the needle position through the voltage profiles applied to the piezo stack [8]. The complete injection system is electronically controlled by the ECU and all the settings are introduced digitally.

The High pressure and high temperature test rig

The tests have been performed in a high temperature and high pressure test chamber where the in-cylinder thermo-dynamic conditions of a Diesel engine at the time of injection can be reproduced. The test chamber allows a maximum ambient temperature of 1000 K and maximum pressure of 15 MPa. The test section has three large optical accesses (128 mm in diameter) placed orthogonally in order to have complete optical access to the injection-atomization. The complete test rig functioning and principles are precisely described in [9].

There are several facilities in the world capable of operating at similar conditions [11][12][13]. Still, this particular test rig is capable of obtaining nearly quiescent, and steady thermodynamic conditions for very long periods of time. This design allows a better (and easier) control and replication of real engine-like test conditions. Its steadier thermodynamic conditions provide a high test repetition rate and quality, improving the global accuracy of the data acquired. In this study, the vessel has been filled with Nitrogen to guarantee the evaporative but non reacting conditions sought.

Optical setup

The Schlieren technique is based on directing a beam of parallel rays of light across a region of interest, collecting this beam and filtering or discarding some of the deflected light, to finally form a shadowgraph in which different pixel intensities acquired represent different refractive indexes in the region of interest.

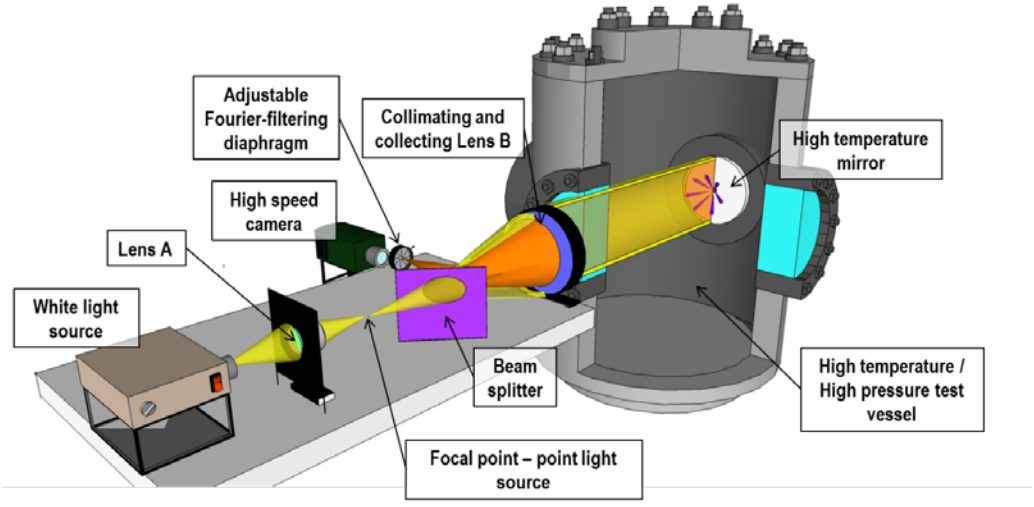

Figure 1 Scheme representing the optical setup.

A scheme of the optical setup is represented in Figure 1. This scheme shows the path of the light throughout the whole setup including the high pressure and high temperature vessel. The yellow translucent beam represents light before reaching the mirror and the orange beam represents light after exiting the test chamber. Being a two pass setup, a mirror inside the test chamber was needed. The beam splitter is used to divide light before and after it has been through the test area. Both the single point light source and the Fourier filtering diaphragm are purposely located at the focal length of Lens B.

The filtering or discarding device utilized in this project consists of an adjustable diameter diaphragm which lets light past its center hole while blocking the rest. This would fall in the category of a circular type cut-off device, which performs symmetrically if everything is properly aligned. The diameter of the center hole is adjustable so it is possible to decide how much light it is desired to go into the camera. This adjustment is what actually controls the system sensibility, by deciding how deflected is the light blocked.

Lens A was introduced to better focus the light source into a smaller and more intensified single point, which is important as it is closely related to the quality of the collimating. The use of just one lens for collimating and collecting (Lens B) was decided in order to reduce to the minimum possible the length of the test area, maximizing so the collection angle.

Table 1 presents the details of the optical setup achieved and the devices utilized in it. The pixel/mm ratio obtained, along with the image size in pixels produce a considerably large image, of approximately 114mm x 114mm. The image size obtained is due to a slight sacrifice in acquisition speed, which could be higher along with a smaller image. Nevertheless, the speed was considered to be enough for the vapor penetration rates involved and the field of view obtained permits the visualization of vapor up to almost the maximum permissible by the window diameter which is 128mm.

Acquisition camera	Phantom V12 CMOS high-speed camera
Acquisition frame rate [frames/second]	14834
Acquisition time step [μs]	67
Camera lens	Nikkor 50mm 1:1.8
Light source	STORZ Xenon NoVA 300
Lens A	Nikkor 50mm 1:1.8
Lens B	TSI f = 450mm
Beam splitter	Edmund Optics 50:50
Mirror	Custom made stainless steel polished mirror
Image size [pixels]	608 x 608
Image pixel/mm ratio [pixel/mm]	5.33
Image size [mm]	114 x 114
Number of repetitions	15

Table 1 Details of the optical setup and devices.

Image processing

The image processing is one of the most important parts of any visualization data analysis [4][14]. Images were processed with purpose developed software. Each image is first divided into 7 sectors, each for one outlet orifice thus one spray. Each spray is processed separately, after masking the image in order to only get the spray of interest. The algorithm details are described in [9]. The image is inverted in order to have the spray as the high luminosity area and the threshold is calculated as the 0.5% of that image's dynamic range [9][15].

Contour analysis: the characteristics of the spray shape are obtained by analyzing its contour. In this work the results related to two macroscopic characteristic of the spray are presented:

- *Maximum vapor penetration VP:* the vapor spray penetration is calculated detecting the point on the contour that is the furthest from the outlet orifice for each of the seven sprays.
- *Spreading angle θ:* a qualitative description of the spreading angle in the first mm of the spray is obtained. The spreading angle is calculated as the angle included between the two lines that fit the points on the spray contour in a specific region, and are forced to go through the outlet orifice. The part of the spray contour that is fitted goes from a 25% to 60% of the spray penetration. The part close to the nozzle outlet is excluded because the whole nozzle itself and its radial isolation ceramic cylinder are non-reflective so no Schlieren effect can be visualized.

Setup limitations

The mirror is essential to the performance of the optical setup. Figure 2 shows an actual image extracted from the camera in which the mirror represents the background.

The three black circles surrounding the center are bolts that hold the mirror against the injector holder. The black centered circle is a hole, needed to fit the injector nozzle and a cylindrical ceramic isolator. The rest of the shades in the picture represent small local density changes which are typically noticeable in high temperature Schlieren setups. These small changes in pixel intensity are not of concern because their velocity is in a completely different order of magnitude than the injection spray itself. Because of this, the background practically remains still during the injection movie and it can be subtracted from the rest of the images. A very small background movement will become evident at the final stages of the injection process but its effect would be easily addressed by the filtering and processing methods.

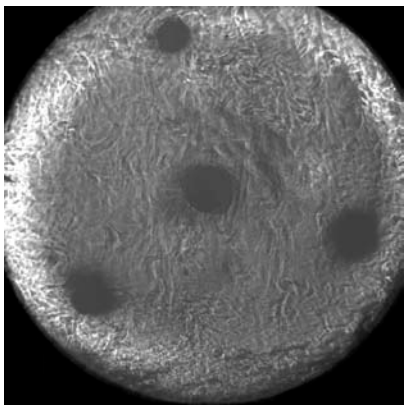

Figure 2 Picture of the mirror and the non-reflective parts. Chamber temperature = 900K.

What actually interrupt spray visualization are the non-reflective parts of the mirror plane; the three bolts that hold the mirror in place and the center hole where the injector nozzle is located. This meant that the clear visualization of three of the seven sprays was disturbed by these bolts, as the sprays traveled over their head diameter. So these three sprays were decided to be excluded from the final averaging, to ensure that the averaging is done from "clean" data. Therefore, results presented regard only the average of four of the seven sprays.

Data averaging

In order to obtain the mean value of the vapor spray penetration and to filter the experimental noise, a moving average technique has been implemented. In each single experiment, a data point y_i is obtained at each instant t_i, time elapsed after the start of the injection. The average value y_m at the instant t_0 is obtained following this procedure:

- The data set falling in the interval $t_0 \pm \Delta t /2$ is considered. An optimal time window (Δt) of 150 μs has been chosen for the current test.
- Over the data set selected, a linear fit is applied and the value of y_m is obtained substituting t_0 in the equation obtained in the linear fit.

This algorithm is repeated moving t_0 along the time line with 15 μs time step; then the averaged curve is obtained.

Experimental test matrix

The test matrix has been designed to understand the effect of partial needle lift in the vapor penetration during both the transient and the steady part of the injection. The test plan has been performed varying the ambient temperature, injection pressure and needle lift and each test point was repeated 15 times. The conditions tested are described in Table 2. As explained before, the maximum needle lift is controlled adjusting the piezo stack charge [8]: the lower the charge, the lower the maximum needle lift.

Parameter	Value	Units
Fuel	Commercial Diesel	-
Orifice diameter	0.152	mm
k-factor	1.5	-
Energizing time	3200	μs
Injector coolant temperature	343	K
Ambient gas pressure	50	bar
Ambient gas temperature	870 - 950	K
Injection pressure	600 - 1500	bar
Piezo stack charge [Ch%]	low-med-high	-
Oxygen concentration	0	%(vol.)

Table 2 Experimental test matrix

Image synchronization

The triggering mode of a fast-camera causes incertitude in the start of the recording. To describe accurately the transient injection this time incertitude has been limited referring all the injection timing to the start of injection (SOI).

It is known that the liquid and vapor penetration curves are not distinguishable at the first part of the injection process [16], so the best approach was to perform a time-alignment of the vapor penetration curves with the previously obtained liquid penetration curves [9] so that they coincide with each other in the early stages of the

injection process. The SOI for liquid penetration has been extrapolated properly in [9], due to a much higher sampling rate along with the visualization setup permitting the acquisition of considerably lower penetration values.

Results and Discussion

The vapor penetration curves (continuous lines) have been plotted over the liquid penetration curves (dashed lines) obtained in [9]. The injector's instant mass flow rates were previously measured in [8] for each case of the test matrix and is also represented in the following curves.

Influence of the ambient temperature

As previously exposed in Table 2, two ambient temperatures were tested, and the effects on vapor penetration were studied. Figure 3 and Figure 4 illustrate the influence of the ambient temperature.

Only the high piezo stack charge case is shown, but all other cases present similar results. As expected, ambient temperature does not affect either the vapor penetration values or the injection rates. The same cannot be said about the liquid penetration which clearly depends on ambient temperature, being the later a determinant factor in the vaporizing process. It is important to remember that the ambient pressure was kept constant at 50 bar so the temperature difference does not cause a significant density variation.

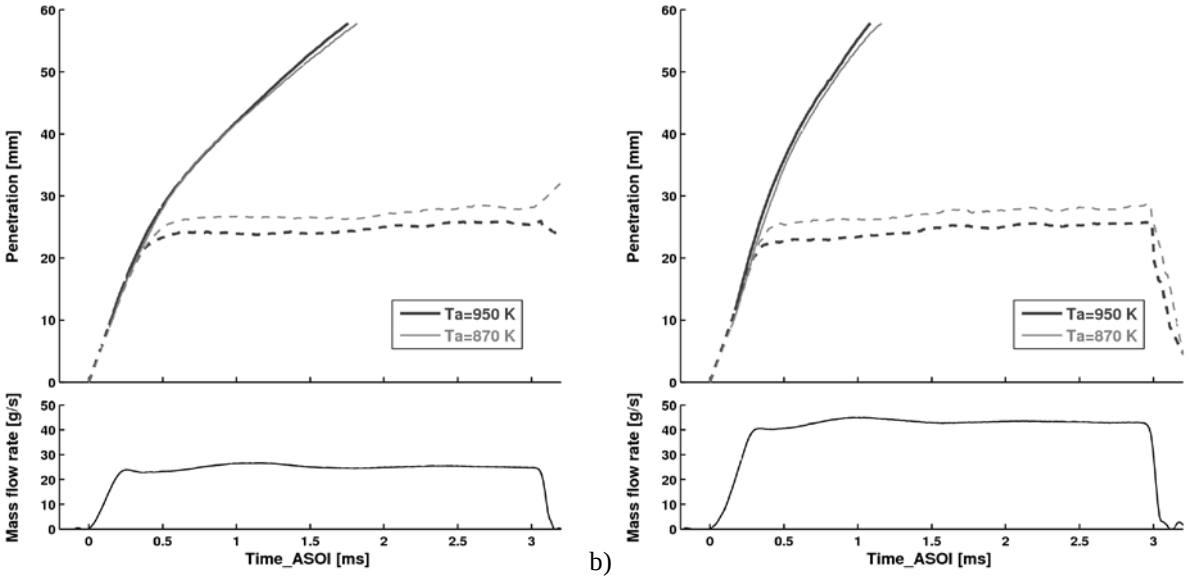

Figure 3 Influence of the ambient temperature in the vapor penetration. a) Pinj = 600 bar, ch% = high. b) Pinj = 1500 bar, ch% = high.

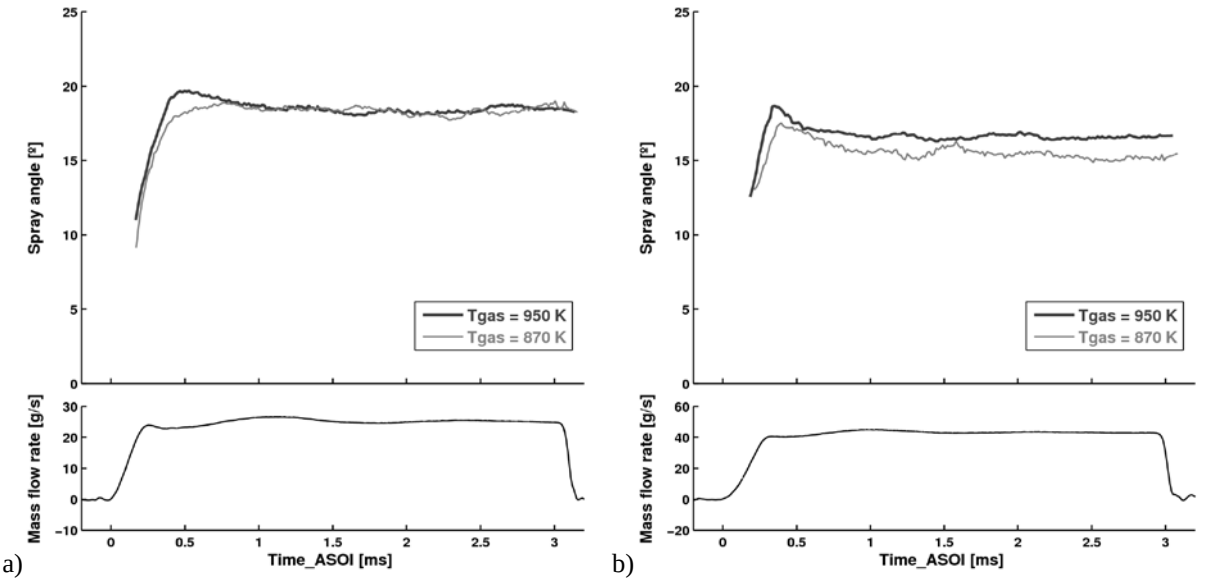

Figure 4 Influence of the ambient temperature in the spreading angle. a) Pinj = 600 bar, ch% = high. b) Pinj = 1500 bar, ch% = high.

Influence of the injection pressure

As previously exposed in Table 2, two injection pressures were tested, and the effects on vapor penetration were studied. Figure 5 and Figure 6 illustrate the influence of the injection pressure:

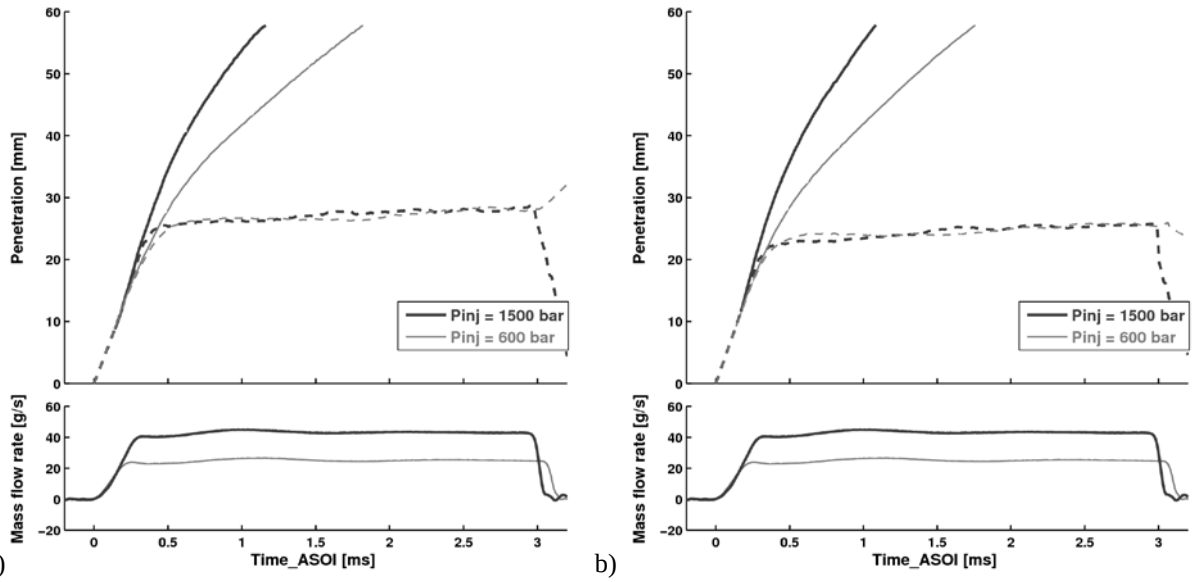

Figure 5 Influence of the injection pressure in the vapor penetration. a) Tamb = 870K, ch% = high. b) Tamb= 950K, ch% = high.

As expected, an increase in injection pressure produces an increase in the vapor penetration rates. These results agree with was previously obtained for the momentum flux and mass flow rates by the authors in [8].

In Figure 6 the results obtained for the spreading angle are presented, it is observed that an increase in the instant injection rate (effective velocity) will cause a decrease in the spreading angle, being both directly related to the injection pressure. In other words, an increase in injection pressure means a decrease in spreading angle.

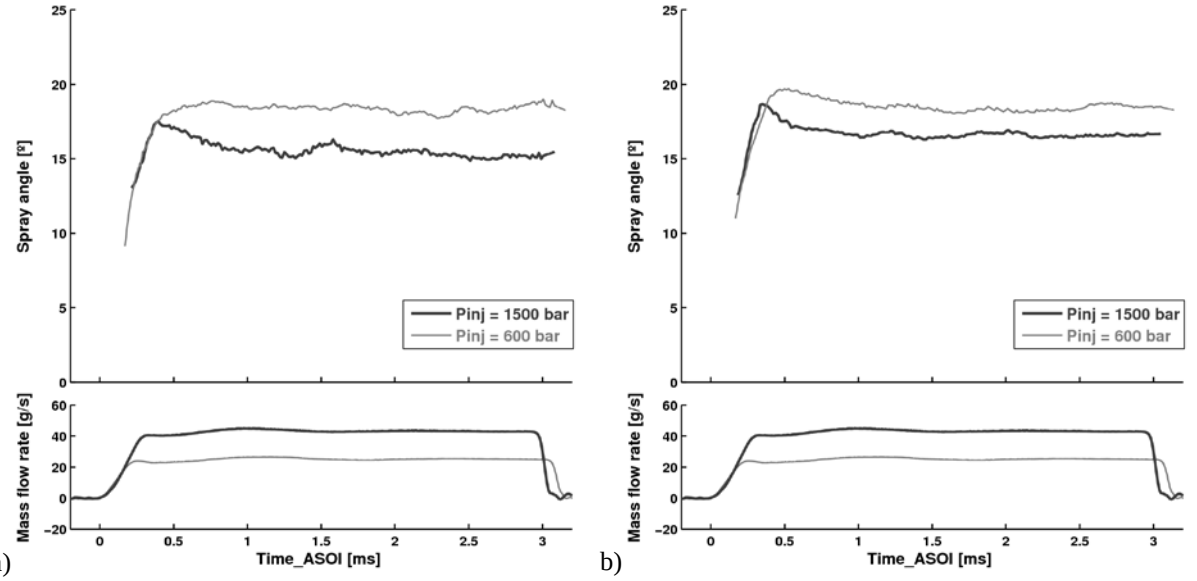

Figure 6 Influence of the injection pressure in the spreading angle. a) Tamb = 870K, ch% = high. b) Tamb= 950K, ch% = high.

Influence of the piezo stack charge

As previously exposed in Table 2, three different piezo stack charge levels were tested, and the effects on vapor penetration were studied. Figure 7 and Figure 8 illustrate the influence of the piezo stack charge.

In this case, only the high temperature case is presented, although the other case shows similar results. Furthermore, it has been seen that temperature does not play a key part in the vapor spray development. The influence of the piezo stack charge is clearly visible in Figure 7. Its effect is similar to that of the injection pressure:

increasing the stabilization value of the injection rate thus increasing vapor penetration rate. This, again, agrees to what the authors found in [8], where the momentum flux of the injection spray increased with the piezo stack charge.

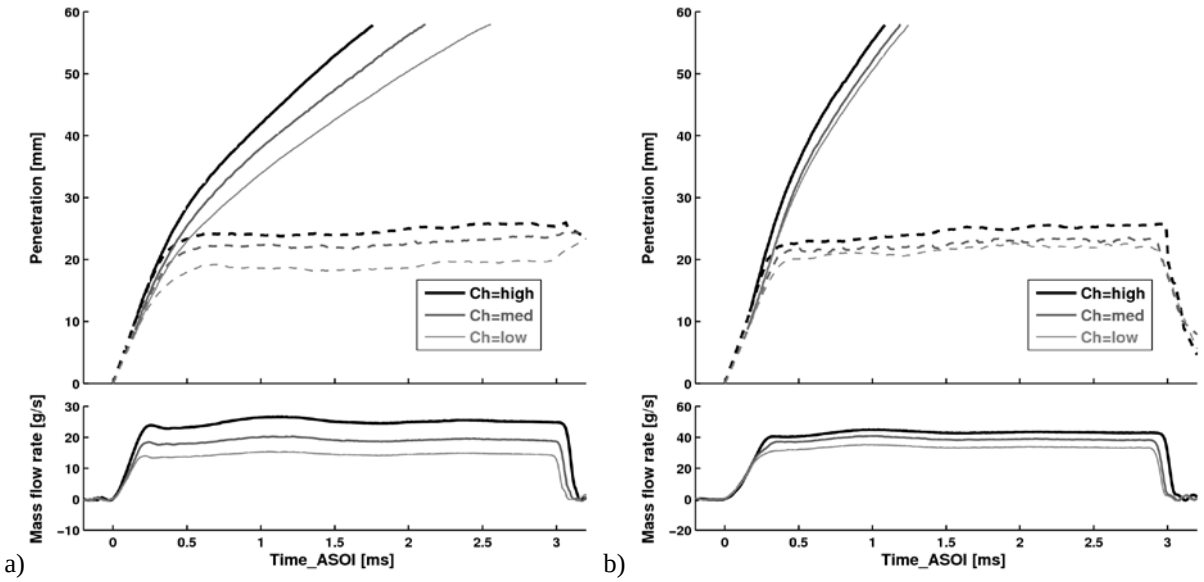

Figure 7 Influence of the piezo stack charge in the vapor penetration. a) Tamb = 950K, Pinj = 600 bar. b) Tamb = 950K, Pinj = 1500 bar,

The effect of the piezo stack charge in the spreading angle is easily noticeable in Figure 8. As in the vapor penetration case, the piezo stack charge effect is very similar to that of the injection pressure. An increase in the piezo stack charge, which is in fact an increase in the needle lift position, produces a decrease in the spreading angle.

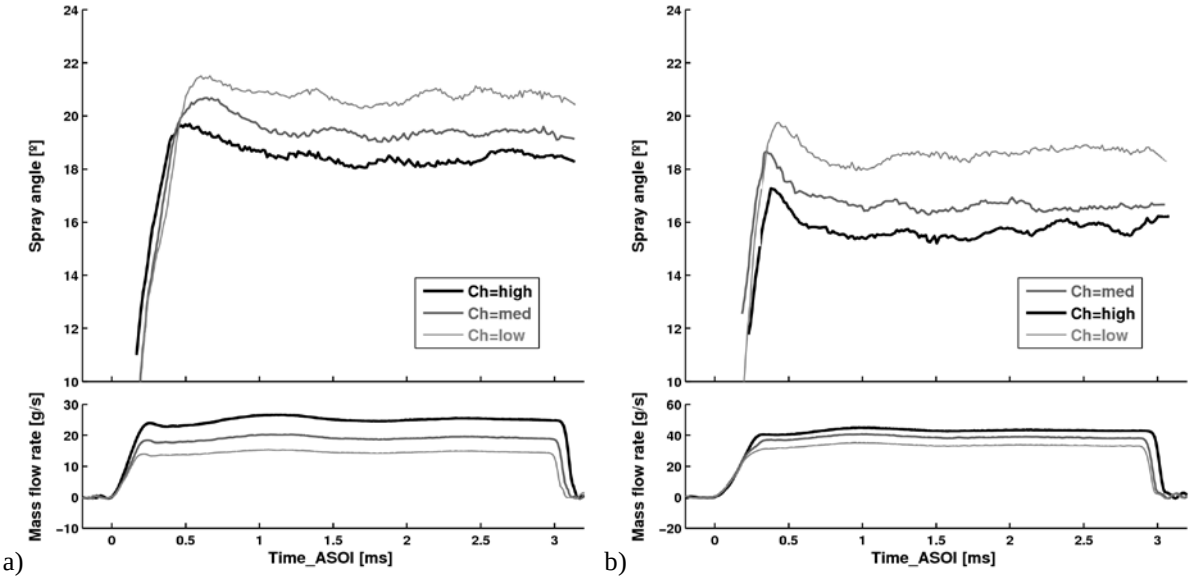

Figure 8 Influence of the piezo stack charge in the spreading angle. a) Tamb = 950K, Pinj = 600 bar. b) Tamb = 950K, Pinj = 1500 bar.

Summary and Conclusions

The influences of ambient temperature, injection pressure and piezo stack charge level were studied. Results show that the piezo stack charge and injection pressure affect the vapor penetration and spreading angle in a similar way. This was expected due to the results presented in [8]. Ambient temperature alone seems not to have an important effect on vapor penetration and spreading angle.

The spray penetration rate is a key factor in the combustion process, for it has a great influence in the air utilization [17]. With these results it is possible to say that engine designers could now control the vapor penetration rate not only with the injection pressures but also with the piezo stack charge. The relationship of both the vapor penetration and the spreading angle to piezo stack charge level leaves room to think that these two variables could easily be controlled as desired through the injection rate profile, which is in fact a unique feature of this prototype injector.

In the end, these results also open room for new questions such as how a particular injection rate profile would affect both the liquid and vapor penetrations. In any case, it has been seen already that this needle lift control feature of the new injector introduces a great potential for engine design and optimization.

Acknowledgments

The authors would like to thank General Motors Company for their financial support and its cooperation during the project and José Enrique del Rey* and Michele Bardi* for their collaboration in the experimental measurements and setup.

(*) From CMT-Motores Térmicos. Universidad Politécnica de Valencia.

References

[1] Soid S.N.; Zainal Z. A.**,** *Spray and combustion characterization for internal combustion engines using optical measuring techniques - A review*, ENERGY, Volume: 36 (2), pp 724-741 (2011).

[2] Payri, R., Salvador, F.J., Gimeno. J., De la Morena, J., *Influence of injector technology on injection and combustion development – Part 1: Hydraulic characterization*, Appl. Energy, pp. 1068-1074 (2011).

[3] Payri, R., Salvador, F.J., Gimeno. J., De la Morena, J., *Influence of injector technology on injection and combustion development – Part 2: Combustion analysis*, Appl. Energy, Vol 88 (4), pp. 1130-1139 (2011).

[4] Siebers D.L., *Liquid-Phase Fuel Penetration in Diesel Sprays*, SAE Paper 980809 (1998).

[5] Myong K, Arai M, Suzuki H, Senda J, Fujimoto H., *Vaporization Characteristics and Liquid-Phase Penetration for Multi-Component Fuels*, SAE 2004-01-0529 (2004).

[6] Ramos, J., *Internal combustion engine modelling*, Hemisphere publishing corporation, ISBN 0-89116-157-0 (1989).

[7] Som, S Ramirez, A.I., Longman, D.E., Aggarwal, S.K., *Effect of nozzle orifice geometry on spray, combustion, and emission characteristics under diesel engine conditions*, FUEL 90 (3), pp. 1267-1276 (2011).

[8] Payri, R., Gimeno, J., Venegas, O., Plazas, A.H., *Effect of Partial Needle Lift on the Nozzle Flow in Diesel Fuel Injectors*, SAE 2011-01-1827 (2011).

[9] Payri, R., Gimeno, J., Bardi, M. Plazas, A.H., *Effect of injection rate shaping over diesel spray development in non reacting evaporative conditions*, ASME ICES2012-81206 (2012).

[10] Som, S., Aggarwal, S.K., El-Hannouny, E.M., Longman, D.E, *Investigation of Nozzle Flow and Cavitation Characteristics in a Diesel Injector*, JOURNAL OF ENGINEERING FOR GAS TURBINES AND POWER-TRANSACTIONS OF THE ASME, Vol 132 (4) (2010).

[11] Baert, R., Frijters, P., Somers, B., Luijten, C., *Design and operation of a high pressure, high temperature cell for HD diesel spray diagnostics: guidelines and results*, SAE Paper 2009-01-0649 (2009).

[12] Pickett, L., Genzale, C.L., Manin, J., Malbec, L-M, Hermant, L., *Measurement Uncertainty of Liquid Penetration in Evaporating Diesel Sprays*, ILASS2011-111 (2011).

[13] Parrish, S. E., Zink, R., *Development and application of an imaging system to evaluate liquid and vapor envelopes of sprays from a multi-hole gasoline fuel injector operating under engine-like conditions*, ILASS2011-170 (2011).

[14] Macian, V., Payri, R., Garcia, A., Bardi, M., *Experimental Evaluation of the Best Approach for Diesel Spray Images Segmentation*, Experimental Techniques doi: 10.1111/j.1747-1567.2011.00730.x (2011).

[15] Siebers, D.L., *Scaling liquid-phase fuel penetration in Diesel sprays based on mixing-limited vaporization*, SAE-1999-01-0528 (1999).

[16] Pastor, J.V., Payri, R., García-Oliver, J.M. and Briceño, F.J., *Analysis of transient liquid and vapor phase penetration for diesel sprays under variable injection conditions*, Atomization and Sprays, 21 (6): 503–520 (2011).

[17] Kook S, Pickett L.M., *Liquid length and vapor penetration of conventional, Fischer–Tropsch, coal-derived, and surrogate fuel sprays at high-temperature and high-pressure ambient conditions*. Fuel, 93, 539-548 (2012).